Biological Psychiatry

Archival Report

# Structural Brain Network Alterations in Relation to Treatment and Illness Severity in Bipolar Disorder

Leila Nabulsi, Melody J.Y. Kang, Neda Jahanshad, Genevieve McPhilemy, Fiona M. Martyn, Bartholomeus Haarman, Colm McDonald, Brian Hallahan, Stefani O'Donoghue, Dan J. Stein, Fleur M. Howells, Freda Scheffler, Henk S. Temmingh, David C. Glahn, Amanda Rodrigue, Edith Pomarol-Clotet, Eduard Vieta, Joaquim Radua, Raymond Salvador, Andriana Karuk, Erick J. Canales-Rodríguez, Josselin Houenou, Pauline Favre, Mircea Polosan, Arnaud Pouchon, Paolo Brambilla, Marcella Bellani, Philip B. Mitchell, Gloria Roberts, Udo Dannlowski, Tiana Borgers, Susanne Meinert, Kira Flinkenflügel, Jonathan Repple, Elisabeth J. Leehr, Dominik Grotegerd, Tim Hahn, Michèle Wessa, Mary L. Phillips, Lea Teutenberg, Tilo Kircher, Benjamin Straube, Olaf Steinstraeter, Frederike Stein, Florian Thomas-Odenthal, Nina Alexander, Paula L. Usemann, Andreas Jansen, Michael Berk, Orwa Dandash, Nadine Parker, Chao Suo, Sophia I. Thomopoulos, Paul M. Thompson, Ole A. Andreassen, Christopher R.K. Ching, and Dara M. Cannon, for the ENIGMA Bipolar Disorder Working Group

## ABSTRACT

**BACKGROUND:** Large-scale T1-weighted magnetic resonance imaging (MRI) studies have established gray matter abnormalities in bipolar disorder (BD), with our group contributing to consensus findings. However, structural connectivity, particularly within emotion- and reward-related circuits, remains poorly understood. Diffusion-weighted MRI (dMRI) enables investigation of white matter pathways, but prior work is constrained by small samples, methodological heterogeneity, and unclear medication effects. We conducted the largest dMRI network analysis in BD, relating symptom burden and polypharmacy to tractography-derived connectivity and graph-theoretical metrics.

**METHODS:** Cross-sectional structural and diffusion MRI scans from 450 individuals with BD (mean ± SD = 35.7 ± 12.6 years) and 509 control participants (33.3 ± 12.6 years), ages 18 to 65 years, were analyzed across 16 ENIGMA (Enhancing Neuro Imaging Genetics through Meta Analysis) BD sites. Standardized segmentation/parcellation and constrained spherical deconvolution tractography generated individual structural connectivity matrices. Graph-theoretical metrics of global and subnetwork organization were related to symptom severity and medications.

**RESULTS:** BD showed widespread network alterations (lower density and efficiency, longer path length, and higher betweenness centrality), altered microstructural organization in a limbic–basal ganglia circuit, and abnormal streamline counts in a default mode/salience/frontolimbic–basal ganglia network. Longer illness duration, later onset, and psychosis history were associated with greater abnormalities in network architecture, whereas more manic episodes were associated with greater frontolimbic connectivity. Antidepressant (particularly selective serotonin reuptake inhibitor), anticonvulsant, and antipsychotic use related to poorer global and frontolimbic connectivity; no clear lithium effects emerged.

**CONCLUSIONS:** As the largest structural connectivity study in BD, we revealed widespread disruption in reward and emotion-regulation networks influenced by illness severity and medication use. Results show that multisite harmonization is feasible and highlight ENIGMA-BD as a scalable framework for identifying reproducible neurobiological markers.

https://doi.org/10.1016/j.biopsych.2026.04.020

Bipolar disorder (BD) is a chronic, recurrent mood disorder characterized by depression and (hypo)mania affecting approximately 1 in 25 adults in the United States and contributing substantially to global disability (1). Although cognitive and affective impairments are well documented, treatment response remains highly variable: Only ∼30% of patients respond robustly to lithium—the standard first-line agent (2)—and many continue to experience persistent


© 2026 Society of Biological Psychiatry. This is an open access article under the CC BY-NC-ND license (http://creativecommons.org/licenses/by-nc-nd/4.0/).

ISSN: 0006-3223

symptoms, functional impairment, or treatment resistance (3,4). BD also carries one of the highest suicide rates among psychiatric disorders (5). Therefore, mapping neural circuit dysfunction is critical for understanding illness burden, predicting treatment response, and advancing biologically grounded, personalized strategies.

BD is characterized by dysregulation within frontolimbic circuits and disrupted interactions with networks supporting fear, anxiety, and cognitive control (6,7). Diffusion-weighted magnetic resonance imaging (MRI) studies show that white matter (WM) abnormalities extend beyond anterior frontolimbic pathways to major association and projection fibers, including the superior longitudinal (arcuate), inferior longitudinal, and inferior fronto-occipital fasciculi; posterior thalamic radiations; and internal capsule (8,9). Robust effects are also observed in the corpus callosum and cingulum, where severity relates to age of onset and illness duration (8), although the contribution of callosal transfer to mood switching and emotional regulation remains unclear (10,11). Altered connectivity in posterior and cerebellar pathways may reflect compensation for disrupted frontal circuits (12). WM disruptions are particularly pronounced in psychotic BD presentations (13) and may contribute to impaired cognitive control and affective instability.

Network neuroscience reframes brain function from regional localization to connectivity-based models, emphasizing distributed interactions among neural systems. Graph theory provides a mathematical framework for this approach, representing regions as nodes and WM pathways as edges, enabling quantification of network organization and integration (14). Although diffusion and structural imaging studies report focal WM abnormalities in BD (15), prior graph-theoretical work has relied on small samples with heterogeneous pipelines, leading to inconsistent network findings. Variability in acquisition, segmentation, parcellation, and connectivity metrics, as well as differences in illness duration, severity, and medication exposure, further contributes to these discrepancies. Large-scale, harmonized network analyses that control for site effects are needed to generate more reproducible estimates of BD circuitry, clarify illness-related variation, and determine how common treatments shape network architecture.

Most patients with BD require concurrent use of multiple medications (polypharmacy) to manage symptoms. Large multisite studies from the ENIGMA (Enhancing Neuro Imaging Genetics through Meta Analysis) BD Working Group have reported associations between psychotropic medications and structural brain features, linking lithium to greater cortical thickness in parietal and frontal regions and anticonvulsants and antipsychotics to thinner cortex and lower surface area in occipital and frontal regions (16,17). In the first ENIGMA-BD diffusion-weighted MRI (dMRI) study ($N$ = 3033; 26 sites), Favre *et al.* (8) found, using diffusion tensor imaging (DTI), that lithium associated with higher fractional anisotropy (FA) and lower mean diffusivity, while antipsychotics and anticonvulsants linked to lower FA. Similar analyses using advanced WM connectivity features such as graph theory are needed to clarify relationships between network dysfunction, treatment, and illness severity in BD.

ENIGMA-BD is the largest global consortium for harmonized neuroimaging and clinical data in BD, enabling standardized processing and improved replicability of brain signatures (18). Using a standardized pipeline across 16 ENIGMA-BD datasets (Figure S1), we assessed whole-brain and subnetwork structural connectivity in individuals with BD versus control participants. Structural connectivity can be quantified using complementary weighting schemes that capture different aspects of WM organization. FA-weighted networks reflect microstructural properties of WM pathways, such as axonal coherence and myelination, whereas networks weighted by the number of streamlines (NOS) represent tractography-derived estimates of connection density (19,20). Each metric provides complementary insights into microstructure organizational properties as they are arranged in large-scale architectural patterns of connectivity of structural brain networks (20). We hypothesized that BD would show network-level disruptions: reduced clustering and efficiency, longer characteristic paths, and higher betweenness centrality, alongside alterations in limbic, basal ganglia, interhemispheric, and cerebellar projections (8,12,21). Furthermore, we predicted that greater symptom burden would relate to more pronounced abnormalities (8) and that medication exposure, particularly to lithium, anticonvulsants, and antipsychotics (especially when categorized by pharmacological mechanisms of action), would account for additional variance in WM network organization, consistent with prior ENIGMA findings (8,16,17). Overall, our goal was to examine the relationships between network metrics, treatment responses, and symptoms to advance the current understanding of BD-related structural networks and identify biologically grounded targets for interventions.

## METHODS AND MATERIALS

### Participants

Sixteen independent ENIGMA-BD cohorts contributed 959 participants (450 BD, 509 control; 51.1% female), ages 18 to 65 years, with DSM-IV-R diagnoses of bipolar I disorder (BDI) or bipolar II disorder (BDII) confirmed by clinical interview with a psychiatrist (demographics and clinical details in Table 1 and Table S2). Individuals with BDI ($n$ = 201) and BDII ($n$ = 42) were included in the analysis when diagnostic subtype information was available. For several cohorts, subtype classification was not consistently reported in the harmonized dataset, resulting in a proportion of participants with BD without subtype specification. These individuals were retained in the primary analyses to maximize sample size, and follow-up tests were conducted in the subset with available subtype information to

**Table 1. Clinical and Sociodemographic Characteristics of Participants**

| | Control, $n$ = 509 | Bipolar Disorder, $n$ = 450 | Statistical Comparison Diagnostic Groups |
|---|---|---|---|
| Age, Years | 33.25 ± 12.61 | 35.65 ± 12.59 | $t_{943}$ = 2.9, $p$ = .003 |
| Sex | | | |
| Female | 281 (55%) | 209 (46%) | $\chi^2_1$ = 6.9, $p$ = .008 |
| Male | 228 (45%) | 241 (54%) | |

Values are presented as mean ± SD or $n$ (%).

examine BDI and BDII differences. Analyses focused on adults, ages 18 to 65, an age range that has been commonly used in prior studies and best represented across sites; participants younger <18 or >65 years or with poor-quality MRI data after inspection were excluded from our analyses. Site-specific inclusion/exclusion criteria are detailed in Table S3. All participating sites obtained approval from their local institutional review boards and ethics committees, and all study participants provided written informed consent.

## Image Acquisition and Processing

Contributing sites shared raw T1-weighted and dMRI scans with the central processing team (acquisition parameters in Table S4). Participant-specific cortico-subcortical brain networks were mapped probabilistically across 86 regions—34 cortical and 9 subcortical bilaterally plus the cerebellum—using FreeSurfer version 5.3.0 (22), with the Desikan-Killiany atlas (23) applied to the T1-weighted images (Figure 1). Diffusion MR images were processed using deterministic constrained spherical deconvolution to resolve crossing fibers (ExploreDTI version 4.8.6) (24,25), as described in Nabulsi *et al.* (21,26) and detailed in the Supplement. Structural connectivity matrices (86 × 86) were weighted by FA and streamline count (NOS); binary matrices were also derived. Network topology was examined across BD and control groups using FA- and NOS-weighted and unweighted matrices.

## Whole-Brain Measures Derived From the Connectome

Global parameters summarizing whole-brain connectivity properties were extracted from both unweighted and weighted matrices (Figure 1). Measures of segregation, including global density and clustering coefficients, were computed as the mean of the respective 86 regional estimates using functions from the Brain Connectivity Toolbox version 1.52 (27). Measures of integration such as characteristic path length and efficiency were derived, as well as measures of influence and centrality, global degree/strength, and betweenness (detailed in Table S5).

## Statistical Analysis of the Structural Connectome

Linear mixed models assessed relationships between whole-brain normally distributed measures and diagnosis, while adjusting for age, sex, and site. In this model, diagnosis, age, and sex were included as fixed effects, and site was included as a random intercept to account for between-site variability (R version 4.2.1) (Figure 1). Age-by-diagnosis and sex-by-diagnosis interactions were also tested. False discovery rate (FDR) correction ($p_{FDR} < .05$) (28) was applied across all tests, consistent with prior graph theory work (19,28). We performed mass univariate testing on FA- and NOS-weighted connectivity graphs using NBS version 1.2 (29) (Figure 1), identifying subgraphs with significantly weaker or stronger connectivity while controlling for familywise error rate (FWER). An *F* test adjusting for age, sex, and site tested group connectivity differences (mean = 5000, $p < .05$); connections were thresholded to retain only suprathreshold edges, with FWER correction via permutation testing ensuring validity regardless of threshold choice (29).

## Clinical Associations in BD

Connectivity associations with clinical variables were tested in the BD group using linear mixed-effects models ($p_{FDR} < .05$). For illness duration and age at onset, age was residualized to isolate effects from age-related influences. Polypharmacy was examined under 2 frameworks: 1) conventional indication-based categories (lithium, antipsychotics, antidepressants, anticonvulsants) (Table S1) and 2) Neuroscience-based Nomenclature (NbN) (30), which classifies medications by neurobiological targets, using medication names or

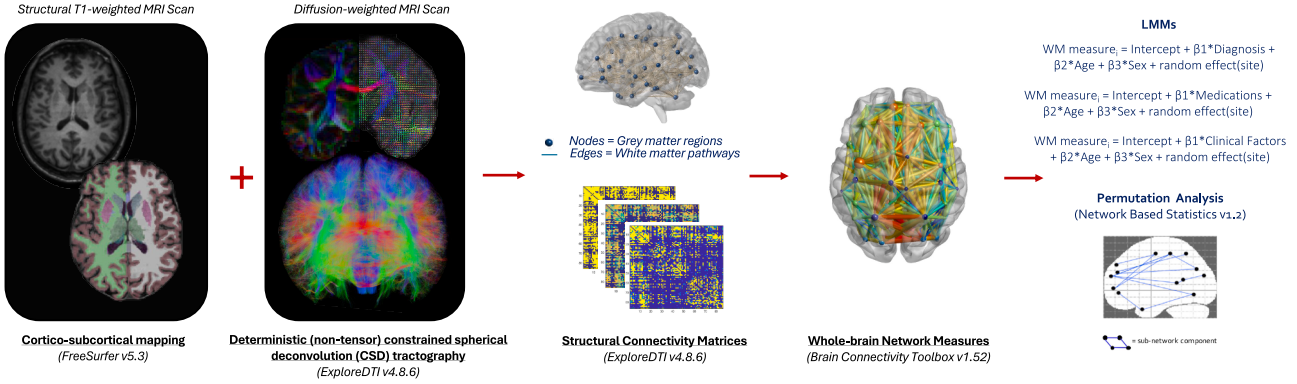



**Figure 1.** Human connectome reconstruction. This figure illustrates the standardized process of human connectome reconstruction and subsequent analyses. Left to right: brain region definition (node): The brain was divided into 34 cortical and 9 subcortical regions bilaterally using FreeSurfer version 5.3.0, based on the Desikan-Killiany atlas. White matter (WM) trajectory reconstruction (edge): White matter pathways were reconstructed using a deterministic nontensor constrained spherical deconvolution algorithm, implemented via ExploreDTI version 4.8.6. Brain network construction: The resulting brain network, composed of nodes and edges (human connectome), is represented as a structural connectivity matrix. Matrices are both unweighted and weighted by fractional anisotropy or the number of streamlines, generated using ExploreDTI version 4.8.6. Global network measures: From the structural connectivity matrices, whole-brain network measures describing features of segregation and integration were calculated using the Brain Connectivity Toolbox version 1.52. Linear mixed models were fitted to investigate structural connectivity differences and the influence of medications and clinical variables; a permutation analysis was performed to identify subnetwork-level differences between patients and control participants using NBS version 1.2 (29). MRI, magnetic resonance imaging.

Anatomical Therapeutic Chemical codes (Table S6). Primary analyses focused on illness duration, age at onset, and lithium, anticonvulsant, and antipsychotic use; exploratory models included symptom severity variables (e.g., psychosis history, episode counts) and NbN categories. All clinical models tested whether effects persisted when controlling for medication use, while medication models adjusted for concurrent medications (polypharmacy) and illness course severity (the number of manic and depressive episodes), ensuring distinct contributions of clinical and pharmacological factors. Model specifications are provided in Table S7.

## RESULTS

### Participants' Clinical and Demographic Characteristics

Individuals with BD were predominantly euthymic (86%) at the time of scanning, significantly older than control participants, and comprised a higher proportion of males (54%) (Table 1). Clinical and sociodemographic details of participants with BD are provided in Table S8.

### Whole-Brain Measures of Network Integration and Segregation

Participants with BD and control participants differed significantly in integration and segregation connectivity metrics (Figure 2 and Table 2). Unweighted network topology in BD showed lower density, longer characteristic path length, lower global efficiency, and higher betweenness centrality (Cohen's $d = -0.2$ to 0.2, $p_{FDR} = .01–.04$). Similar disruptions were observed in NOS-weighted networks, with longer path length and lower efficiency in BD ($d = 0.2$, $p_{FDR} = .001$), while FA-weighted networks showed no group differences. Males showed lower clustering and local efficiency ($d = -0.3$, $p_{FDR} = .0002$) than females in NOS-weighted networks independent of diagnosis, with no sex-by-diagnosis interaction. Age was significantly associated with lower density and efficiency (unweighted) and with path length, local efficiency, and betweenness centrality (NOS weighted) ($p_{FDR} = .007–.03$), but no age-by-diagnosis interaction was detected ($p_{FDR} = .8–.9$). A sorted bar plot of Cohen's $d$ effect sizes for whole-brain network metrics is provided in Figure S2.

### Permutation-Based Subnetwork Analysis

Edge-level analysis identified a differentially connected subnetwork (FA-weighted) in participants with BD relative to control participants ($t > 1.5$, $d = 0.2$, $p_{FWE} = .0002$) involving 27 structural dysconnections predominantly between and within limbic and basal ganglia nodes and cerebellar connections via limbic system nodes (Figure 3 and Table S9). A differentially connected subnetwork (NOS-weighted) was also seen for participants with BD relative to control participants ($t > 10$, $d = 0.5$, $p_{FWE} = .005$) involving 37 structural dysconnections encompassing connections between default mode/salience network nodes and frontolimbic system and basal ganglia nodes (Figure 3 and Table S10). No significant (FA/NOS-weighted) weaker/stronger subnetwork was identified when we compared males with females or when we tested for a diagnosis-by-sex interaction.

### Clinical Associations Within the BD Group

At the whole-brain level, longer illness duration (mean ± SD = 16 ± 11 years) was associated with lower network density, efficiency, and longer path length (Figure S3A). Later illness onset (21 ± 9 years) was linked to longer path length and poorer efficiency (Figure S3B). A history of psychosis ($n = 116$) was associated with lower density, longer path length, and higher betweenness centrality compared with those without a psychosis

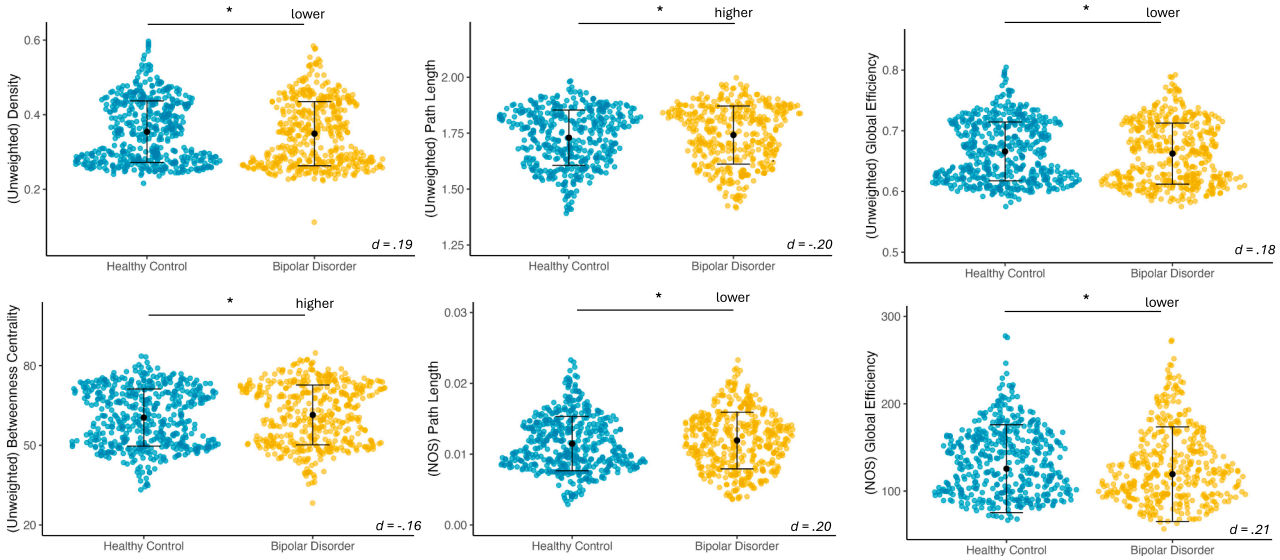



**Figure 2.** Whole-brain measures affected in bipolar disorder (BD). Global network measures affected in the BD group relative to the control group. The BD group exhibited dysconnectivity compared with the healthy control group across unweighted and number of streamlines (NOS)–weighted networks. Dysconnectivity was defined by lower global density, longer path length, and lower global efficiency. Bars represent mean ± SD; raw means are plotted. *False discovery rate–corrected $p < .05$

**Table 2. Global Network Measures Across Unweighted and Weighted Networks**

| Network Metric | Healthy Control, $n$ = 509 | Bipolar Disorder, $n$ = 450 | $p_{FDR}$ | Cohen's $d$ |
|---|---|---|---|---|
| Binary Density | 0.354 ± 0.082 | 0.349 ± 0.086 | .018* | 0.19 |
| Binary Degree | 48.685 ± 37.111 | 48.690 ± 37.222 | .666 | −0.04 |
| Binary Clustering Coefficient | 0.652 ± 0.036 | 0.648 ± 0.045 | .786 | 0.03 |
| Binary Characteristic Path Length | 1.527 ± 0.567 | 1.541 ± 0.568 | .018* | −0.20 |
| Binary Global Efficiency | 0.666 ± 0.049 | 0.662 ± 0.050 | .021* | 0.18 |
| Binary Local Efficiency | 0.927 ± 0.008 | 0.927 ± 0.008 | .067 | 0.15 |
| Binary Betweenness Centrality | 60.461 ± 10.763 | 61.450 ± 11.265 | .042* | −0.16 |
| FA Strength | 12.323 ± 9.527 | 12.094 ± 9.486 | .121 | 0.12 |
| FA Clustering Coefficient | 0.247 ± 0.165 | 0.246 ± 0.163 | .138 | 0.11 |
| FA Characteristic Path Length | 4.810 ± 1.441 | 4.861 ± 1.430 | .397 | −0.07 |
| FA Global Efficiency | 0.288 ± 0.162 | 0.281 ± 0.162 | .946 | 0.01 |
| FA Local Efficiency | 0.345 ± 0.220 | 0.347 ± 0.218 | .367 | 0.08 |
| FA Betweenness Centrality | 80.308 ± 20.387 | 81.264 ± 19.584 | .369 | −0.07 |
| NOS Strength | 2728.270 ± 981.834 | 2583.344 ± 1014.681 | .090 | 0.13 |
| NOS Clustering Coefficient | 35.332 ± 8.302 | 33.635 ± 7.587 | .987 | 0.00 |
| NOS Characteristic Path Length | 0.011 ± 0.004 | 0.012 ± 0.004 | .018* | −0.20 |
| NOS Global Efficiency | 125.679 ± 50.367 | 119.366 ± 54.184 | .018* | 0.21 |
| NOS Local Efficiency | 62.883 ± 14.794 | 59.982 ± 13.883 | .786 | 0.03 |
| NOS Betweenness Centrality | 166.410 ± 25.291 | 167.660 ± 26.574 | .090 | −0.14 |

Values are presented as mean ± SD. Measures are shown across unweighted (binary) networks, with diagnostic group differences in global density, path length, efficiency, betweenness centrality, and weighted networks.

*$p_{FDR} < .05$.

FA, fractional anisotropy; FDR, false discovery rate; NOS, number of streamlines.

diagnosis ($n$ = 112) (Figure S3C). All associations remained significant after adjusting for medication use, apart from illness duration effects on centrality. The number of manic or depressive episodes showed no significant associations with global metrics ($p_{FDR} > .05$). Statistical details are provided in Table S11.

In subnetwork analyses, longer illness duration was linked to lower FA-weighted connectivity between the right hippocampus and amygdala and lower NOS-weighted connectivity between the right cerebellum and thalamus (Figure S3D and Table S11). Later illness onset was associated with lower NOSs in connections involving the right cerebellum–thalamus, right amygdala–accumbens, right pallidum–insula, amygdala-fusiform, and left amygdala–medial orbitofrontal cortex (Figure S3D). Greater number of manic episodes was associated with higher NOS-weighted connectivity involving the right anterior middle frontal cortex–ventral diencephalon area, while depressive episodes and psychosis history showed no significant subnetwork associations ($p_{FDR} > .05$). Results remained significant after adjusting for medication use. No connectivity (whole brain and subnetwork) differences were observed between diagnostic BDI ($n$ = 201) and BDII ($n$ = 42).

## Treatment Associations

In BD, antidepressant use at the time of scan was associated with lower network density, longer path length, lower efficiency, and higher betweenness centrality at the whole-brain level, even after adjusting for illness severity and concurrent medications (Figure S4). No significant associations were observed for lithium, anticonvulsants, or antipsychotics on global network measures ($p_{FDR} > .05$). At the subnetwork level, anticonvulsant use was associated with higher NOS-weighted connectivity between the right pallidum and both the right ventral diencephalon and the superior frontal cortex and lower connectivity between the right putamen and the medial orbitofrontal cortex (Figure S4). Additional patterns of lower NOS-weighted connectivity were observed between the right thalamus and the fusiform, lingual, and lateral occipital cortices (Figure S4). However, after accounting for illness severity, the associations previously observed with anticonvulsant use were no longer significant. No significant FA/NOS-weighted subnetwork associations were found for lithium, antidepressants, or antipsychotics.

Use of serotonin (5-HT) reuptake inhibitors (NbN4) was associated with lower density, longer path length, lower efficiency, and higher betweenness centrality at the whole-brain level, even after adjusting for illness course severity measures and other NbN-based treatment categories (Figure S4). 5-HT reuptake inhibitor use was also linked to lower FA-weighted connectivity between the right thalamus and the hippocampus (Figure S4), independent of depressive episodes and other medication classes but not manic episodes. Use of dopamine, 5-HT, and noradrenaline receptor antagonists (NbN2) was associated with lower NOS-weighted connectivity between the left and right middle orbitofrontal gyri, even after accounting for illness course severity scores and other NbN categories (Figure S4). Statistical details are provided in Table S11.

## DISCUSSION

Our study represents the largest analysis of brain network organization in BD reported to date, analyzing 450

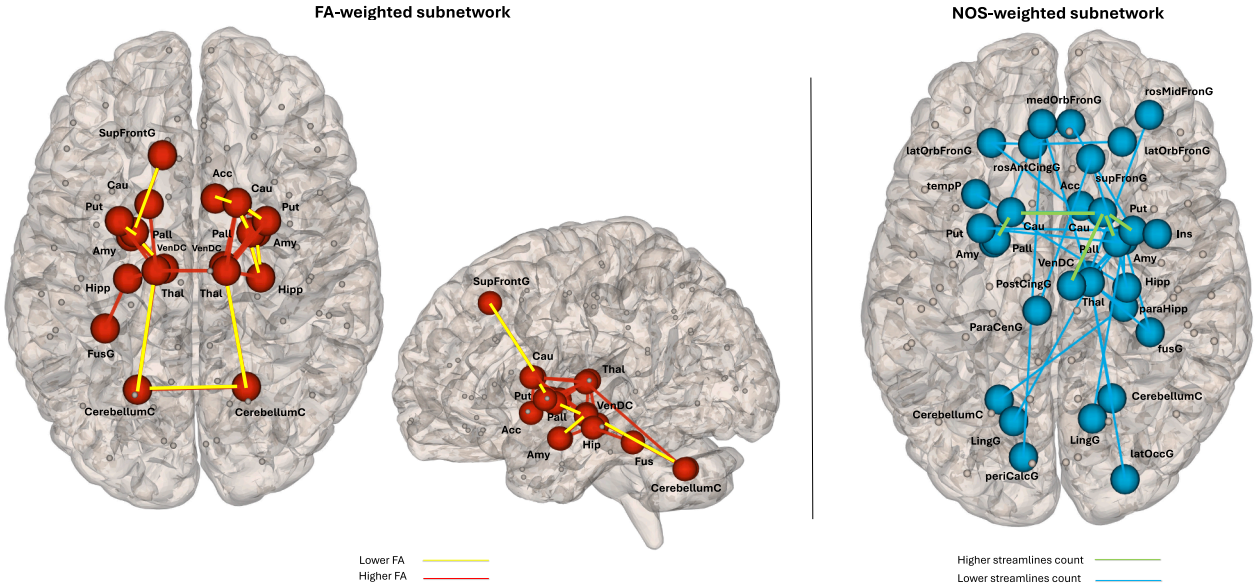



**Figure 3.** Subnetwork graph components showing altered fractional anisotropy (FA)–weighted and number of streamlines (NOS)–weighted connectivity in bipolar disorder (BD). The left panel displays a network of altered FA-weighted connectivity in participants with BD compared with control participants, with the most significant differences observed between and within the basal ganglia and limbic connections ($t > 1.5$, familywise error–corrected $p$ [$p_{FWE}$] = .0002, $d = 0.2$). Connections with lower FA-weighted connectivity are shown in yellow, while those with higher FA-weighted connectivity are depicted in red. The right panel illustrates altered NOS-weighted connectivity in participants with BD vs. control participants ($t > 10$, $p_{FWE} = .005$, $d = 0.5$), primarily involving the default mode/salience network regions, frontolimbic system, and basal ganglia connections. Those connections with lower NOS-weighted connectivity are depicted in blue, while those with higher NOS connectivity are displayed in green. Acc, accumbens; Amy, amygdala; C, cortex; Cau, caudate; FusG, fusiform gyrus; Hipp, hippocampus; Ins, insula; latOccG, lateral occipital gyrus; LingG, lingual gyrus; medOrbFronG, medial orbitofrontal gyrus; Pall, pallidum; paraHipp, parahippocampal gyrus; periCalcG, pericalcarine cortex; PostCingG, posterior cingulate gyrus; Put, putamen; rosAntCingG, rostral anterior cingulate gyrus; rosMidFronG, rostral middle frontal gyrus; supFronG, superior frontal gyrus; tempP, temporal pole; Thal, thalamus; VenDC, ventral diencephalon.

predominantly euthymic individuals with BD relative to 509 control participants across 16 international cohorts. BD was associated with altered whole-brain connectivity and regional dysconnectivity within frontolimbic and basal ganglia pathways and networks linking default mode, salience, and basal ganglia regions. Illness severity measures further modulated these alterations: Longer illness duration and later onset were associated with more pronounced global and subnetwork disruptions, a history of psychosis was associated with greater deviations in global network features, and a greater number of manic episodes was associated with higher frontolimbic connectivity. Pharmacological treatments showed distinct, class-specific associations: Antidepressant use, particularly selective serotonin reuptake inhibitors (SSRIs), was linked to lower global network integration (lower density and efficiency), longer paths, higher centrality, and reduced microstructural organization between key limbic regions, while anticonvulsants and antipsychotics were associated with alterations in basal ganglia–mediated emotion-regulation and cognitive-control circuits, including fewer streamlines between frontal cortices.

Our findings reveal a subtle but reliable pattern of whole-brain dysconnectivity in BD across key measures of network integration and segregation (Figure 2), with the largest group differences emerging for characteristic path length and global efficiency. The magnitude and direction of these effects were comparable to those reported in large-scale meta-analytic work (8), reinforcing the presence of modest but consistent disruptions in global network topology. Lower global density and efficiency indicate weaker large-scale integration, while longer paths and elevated betweenness centrality suggest that information flow becomes less direct and more reliant on a limited set of hubs. This configuration reflects a compromised topological organization in BD, one in which fewer hubs carry a disproportionate share of network communication. Clinically, reduced integration and hub overreliance may contribute to cognitive and affective disturbances (31) and increase vulnerability to destabilization during stress or mood-state transitions, consistent with evidence linking compromised connectivity to episode onset (32–34). These findings are consistent with prior reports of reduced clustering and efficiency and altered hemispheric or regional connectivity (6,35–38), supporting a convergent pattern of global topological abnormalities across studies. We also observed sex-related differences, with males showing lower clustering and local efficiency than females, consistent with prior work on sex-specific connectivity (39,40) and reports of sex-linked cognitive variation in BD (41), although these differences did not extend to subnetwork connectivity in our sample.

Whole-brain alterations in BD were driven primarily by dysconnectivity within 2 subnetworks: 1) frontolimbic and basal ganglia pathways, including posterior cerebellar projections and 2) a network linking default mode, salience, frontolimbic, and basal ganglia regions (Figure 3). The involvement of default mode and salience networks in BD points to potential dysfunction in self-referential processing

and attentional control (42), while across both subnetworks the most pronounced effects involved basal ganglia connections, underscoring their central role in BD-related structural disruption and in emotion regulation, reward processing, and cognitive control. Differences between FA-weighted and streamline-weighted networks suggest complementary microstructural (e.g., axonal density, myelination) and macrostructural (tract-level) alterations (43,44). The co-occurrence of lower and higher connectivity within these subnetworks is consistent with a pattern of both disruption and compensatory reorganization, in which loss of WM microstructure in core affective pathways may be offset by increased reliance on alternative routes to maintain communication. These divergent patterns indicate that BD involves not only structural disruption but also dynamic, potentially compensatory reorganization aimed at preserving communication across affected circuits. Appreciating these network-level adaptations highlights the need to study both structural and dynamic processes and motivates the search for biomarkers that index these compensatory mechanisms, with the potential to guide future circuit-based interventions in BD. Ongoing efforts within ENIGMA are beginning to bridge such MRI-derived patterns with underlying biological gradients, including cell type–specific gene expression and neurotransmitter profiles (45,46). The anatomical distribution of effects aligns with prior BD findings, particularly involving the anterior limb of the internal capsule, uncinate fasciculus, ventral amygdalo-striatal projections, cingulum, fornix, and corpus callosum—tracts that link basal ganglia nodes with limbic, frontal, and diencephalic regions implicated in affective regulation (6,35,37,47). Consistent with the largest multicenter ENIGMA-BD DTI study (8), which reported widespread FA reductions with strongest effects in the corpus callosum and cingulum, our multisite tractography and network-level approach shows how these regional abnormalities converge into systems-level alterations. This shift from isolated regions to distributed networks is crucial, as converging evidence suggests that psychiatric disorders arise from disturbances in network organization (48,49), with direct implications for developing circuit-level, mechanism-based interventions.

Our findings also highlight the salience network's role in BD, particularly its integration with subcortical regions involved in interoception and visceromotor control (50). Within this network, the anterior cingulate cortex occupies a strategic connector-hub position linking the amygdala, orbitofrontal cortex, olfactory cortex, and temporal regions critical for emotion regulation and homeostasis (51). Dynamic instabilities in interoceptive networks may underlie the maladaptive responses to emotional stimuli observed in BD (15) and consequent aberrant perception of emotional stimuli as increasingly salient (52). The elevated betweenness centrality observed in BD, together with prior evidence of altered connector-hub organization (21,52), suggests increased reliance on these hubs to compensate for lower structural connectivity within core affective and interoceptive pathways. Such hub overreliance may reflect compensatory engagement of connector hubs that support the integration of external stimuli with self-referential processing—a process known to be disrupted in BD and other mood disorders (15,53–55)—and may be key to the regulation of emotional experiences in BD.

Clinical features were significantly associated with topological network organization in BD (Figure S3). Longer illness duration was linked to widespread reductions in network integration across large-scale systems, and older individuals with BD showed greater amygdala-hippocampal connectivity alterations, consistent with cumulative disease burden and evidence that chronic neuroinflammatory processes and glial activation contribute to progressive WM abnormalities in BD, although cross-sectional design limits causal inference (56). Later illness onset was associated with more pronounced global topological alterations, particularly within cerebello-thalamic and frontolimbic–basal ganglia pathways including reduced connectivity along uncinate fasciculus–related regions. This association warrants cautious interpretation: Later onset may reflect differences in treatment timing, illness recognition, or underlying biological and clinical factors, including genetic or experiential reserve, that allow individuals to tolerate illness burden before symptom emergence, although these possibilities cannot be directly tested in our cross-sectional design. Notably, earlier onset is often associated with greater clinical severity, and distinct neurobiological subtypes of BD may contribute to variability in illness onset. A history of psychosis was linked to a more fragmented and inefficient global network, consistent with greater reliance on a limited set of high-betweenness nodes to compensate for broader connectivity deficits (57,58). In contrast, a greater number of manic episodes was associated with higher connectivity between the anterior middle frontal cortex and subcortical regions inferior to the thalamus (hypothalamus, mammillary bodies, subthalamic nuclei, substantia nigra), consistent with mania-induced neural plasticity in frontolimbic circuitry via dopaminergic and glutamatergic mechanisms (34,59–61). The absence of similar effects for depressive episodes suggests distinct mood-state–dependent mechanisms, although our predominantly euthymic sample and cross-sectional design may limit detection of acute or residual mood-related structural changes (62). These results demonstrate that illness-related factors (duration, onset age, psychosis history, and episode frequency) must be modeled to understand BD network pathology and motivate longitudinal, deeply phenotyped studies to distinguish illness burden, compensatory reorganization, and cumulative manic effects—a distinction with direct relevance for early, mechanism-guided intervention. Richer phenotypic characterization, including symptom clustering, illness trajectory modeling, and item-level severity measures, may further clarify whether observed alterations reflect shared circuit vulnerability or biologically distinct BD subtypes.

Antidepressant use, particularly of SSRIs, was associated with lower connectivity within limbic circuits involving the thalamus and hippocampus and with reduced global network integration. While SSRIs may help stabilize mood, their mechanism of action could differentially modulate WM connectivity in regions already vulnerable to illness severity in BD. Lower connectivity in specific networks does not necessarily indicate a detrimental effect on brain function. Pharmacological treatments may dampen pathological hyperconnectivity or rebalance circuit dynamics within emotion-regulation networks (63,64). Medication use was not randomly assigned, and although our models accounted for symptom severity and

number of depressive episodes, residual confounding and unmeasured aspects of illness chronicity may persist, particularly among individuals more likely to be prescribed SSRIs. Therefore, connectivity reductions may reflect adaptive modulation rather than structural impairment and may partially reflect differences in underlying symptom-severity profiles difficult to disentangle without item-level measures, an area of ongoing ENIGMA-BD work. ENIGMA studies of major depressive disorder found cortical and hippocampal differences in medicated patients but no WM microstructural changes (65), suggesting that antidepressant-related WM alterations may be BD-specific illness burden dependent. Anticonvulsant use produced mixed connectivity changes within emotion-regulation and cognitive-control circuits overlapping with BD sociocognition networks (32) and regions sensitive to anticonvulsant-related cognitive effects (66); these associations did not survive illness severity adjustment, underscoring the challenge of separating medication effects from disease burden and the need for prospective, dose-resolved longitudinal designs. Antipsychotic use was linked to lower connectivity between the medial orbitofrontal cortex and other frontal regions, potentially reflecting therapeutic modulation of limbic-frontal integration or cognitive side effects, with longitudinal dose-resolved data needed to distinguish these. Lithium and other mood stabilizers did not show clear associations with network connectivity in our sample. This absence may reflect lithium's distinct intracellular signaling mechanisms differing from the receptor- or ion channel–based actions of SSRIs, antipsychotics, and anticonvulsants and is consistent with its proposed neuroprotective influence (16,17), suggesting a stabilizing effect on WM architecture (even if not significant here). The relative preservation of network organization in lithium-treated individuals offers a translational distinction between medications that maintain structural connectivity and those associated with reduced integration, suggesting that connectomic markers could help differentiate treatments by their network impact. Whether this reflects a true mechanistic distinction from other psychotropics or methodological limitations requires further study. Overall, our findings support the notion that psychotropic medications influence network organization in circuits aligned with their mechanistic targets, raising important questions about whether these changes are adaptive, maladaptive, or necessary clinical trade-offs, although longitudinal studies remain essential to disentangle medication effects from illness progression.

Several limitations should be considered. While ENIGMA applies standardized processing pipelines and rigorous quality control procedures (18), and linear mixed-effects models with site as a random effect account for multisite heterogeneity in acquisition parameters and scanner platforms, it is possible that there remains site-related variability. Even so, we note that the heterogeneity is present whether or not the study design models it, and a single site design simply ignores it, by being unable to determine whether the effects are specific to the cohort or whether they generalize to other cohorts. Clinical data were standardized across cohorts to accommodate differences in recruitment strategies, diagnostic assessment procedures, and inclusion/exclusion criteria. Medication exposure was assessed cross-sectionally at the time of scanning, reflecting naturalistic polypharmacy patterns in BD. The number of individuals receiving lithium monotherapy was relatively small and unevenly distributed across cohorts, limiting statistical power for reliable monotherapy analyses.

Future large-scale, treatment-stratified datasets will be needed to clarify medication-specific network effects. As a result, causal inferences regarding treatment effects on structural connectivity cannot be drawn. Finally, diffusion tractography provides indirect WM pathway reconstruction and is sensitive to crossing fibers, algorithmic choices, and threshold parameters (67,68). Despite these limitations, the large, harmonized sample and standardized analytic framework support the generalizability of observed network signatures across diverse sites.

## Conclusions

In the largest BD connectome study to date, we demonstrated the feasibility and value of large-scale, harmonized diffusion MRI connectome analyses, identifying subtle but robust alterations in emotion-regulation and reward-related networks further shaped by illness burden and pharmacological treatment. We report mechanism of action–dependent medication effects, particularly antidepressant-related limbic connectivity alterations, underscoring the importance of accounting for treatment exposure and developing more sophisticated approaches to modeling medication effects when interpreting network abnormalities. More broadly, these results illustrate how network-based approaches capture system-level disruptions not apparent in regional analyses and provide a framework for disentangling pharmacological from core neurobiological features of BD. Although cross-sectional design precludes causal inference and observed connectivity differences likely reflect a combination of disease mechanisms, illness progression, treatment exposure, and environmental influences, the consistent involvement of frontolimbic and reward-related circuits highlights network-level processes relevant to mood regulation and treatment response. Large-scale connectomic studies may identify circuit-level markers to support illness staging, improve treatment stratification, and guide the development of more targeted, circuit-informed therapeutic strategies. Collaborative efforts at this scale will be critical for advancing biomarker discovery and improving the biological understanding of psychiatric disorders.

## ACKNOWLEDGMENTS AND DISCLOSURES

LN was supported by a 2025 NARSAD Young Investigator Grant from the Brain & Behavior Research Foundation (Grant No. 32792) and the Irish Research Council Postgraduate Scholarship. DMC was supported by the Health Research Board (Grant No. HRA-POR-324). GM was supported by the Irish Research Council Postgraduate Scholarship. NJ was supported in part by the National Institutes of Health (NIH) (Grant No. R01MH134004). PMT, SIT, NJ, CRKC, and LN were supported in part by NIH (Grant No. R01MH129742; ENIGMA Bipolar R01 [to PMT and OAA]); EJL, UD, SM, FSt, BS, and TK were supported by the German Research Foundation (DFG) SFB/TRR 393 project (Grant No. 521379614 [to TK and UD]). EJL was supported by Else Kröner-Fresenius-Stiftung (Grant No. 2022_EKEA.193) and the Innovative Medical Research of the medical faculty of the University of Münster (Grant Nos. BÖ112202 and LE112403); UD was supported by DFG (Grant Nos. FOR2107 DA1151/5-1, DA1151/5-2, DA1151/9-1, DA1151/10-1, and DA1151/11-1) and the Interdisciplinary Center for Clinical Research of

the medical faculty of Münster (Grant No. Dan3/022/22 [to UD]). TK and LT were supported by consortia grants from DFG FOR 2107 (DFG Grant Nos. FOR2107 KI588/14-1, KI588/14-2, KI588/20-1, and KI588/22-1). Biosamples and corresponding data were sampled, processed, and stored in the Marburg Biobank CBBMR. BS was supported by consortia grants from DFG extension to the FOR 2107 (DFG Grant No. STR1146/18-1). MP and the Grenoble MRI facility IRMaGe are partially funded by the French program "Investissement d'Avenir" run by the Agence Nationale de la Recherche (Grant Infrastructure d'avenir en Biologie Santé No. ANR-11-INBS-0006). JH was supported by Agence Nationale de la Recherche (Grant Nos. ANR-11-IDEX-0004 Labex BioPsy and ANR-10-COHO-10-01 psyCOH), Fondation pour la Recherche Médicale (Bioinformatique pour la biologie 2014), and Fondation de l'Avenir. AR and DCG were supported by the National Institute of Mental Health (Grant Nos. MH077945, MH106324, and MH080912). PBM was funded by the Australian National Medical and Health Research Council (Grant Nos. 1037196 and 1177991), the Longwood Foundation, Good Talk, and the Keith Pettigrew Family Bequest. OAA was funded by the Research Council of Norway (Grant No. 324499), KG Jebsen Stiftelsen (Grant No. SKGJ-MED-021), NordForsk (Grant No. 164218), and South East Norway Health Authority (Grant No. 2023-031). JRe was supported by the LOEWE program of the Hessian Ministry for Science and the Arts (Grant No. LOEWE1/16/519/03/09.001(0009)/98). MW was supported by grants from the DFG (Grant Nos. We3638/3-1 and We3638/5-1, SFB636/Project C6). AJ was funded by the DFG under Germany's Excellence Strategy (EXC 3066/1 "The Adaptive Mind," Project No. 533717223), within the Research Unit FOR2107 (JA1890/7-1, JA1890/7-2), and within the CRC/TRR 393 "Trajectories of Affective Disorders" (project Grant No. 521379614, projects B01 and INF).

DMC, LN, GM, CM, and BHal acknowledge the participants and the support of the Wellcome Trust Health Research Board Clinical Research Facility and the Centre for Advanced Medical Imaging, St. James Hospital, Dublin, Ireland; DJS, HST, FSc, and FMH acknowledge the University Research Committee, University of Cape Town and South African funding bodies National Research Foundation and Medical Research Council; and Marinka M.G. Koenis for data support (Yale/Olin Cohort).

OAA, MBel, MBer, PB, DMC, CRKC, UD, DCG, DG, BHaa, TH, JH, FMH, TK, CM, PBM, PMT, MLP, MP, EP-C, EV, MW, and HST contributed as cohort principal investigators. LN and DMC contributed as project leaders. LN, DMC, CRKC, MJYK, and PMT contributed to the core analysis/writing group. MBel, MBer, TB, EJC-R, OD, UD, PF, KF, BHal, JH, FMH, AJ, AK, EJL, FMM, CM, GM, SM, PBM, LN, SO, MLP, MP, AP, JRa, JRe, GR, AR, RS, FSc, FSt, OS, CS, HST, LT, FT-O, PLU, GM, DCG, and HST contributed to the clinical data collection. MBel, MBer, TB, EJC-R, OD, UD, PF, KF, JH, FMH, AJ, AK, FMM, GM, CM, SM, PBM, LN, SO, MLP, MP, AP, JRa, JRe, GR, AR, RS, FSc, FSt, OS, CS, HST, LT, FT-O, DCG, JRe, and BS contributed to the imaging data collection. LN, NA, OAA, MBel, CRKC, OD, UD, PF, DCG, TH, JH, FMH, NJ, MJYK, CM, PBM, MP, JRa, GR, DJS, FSt, BS, SIT, PMT, NP, HST, and JRe contributed to article revision/editing.

We would like to acknowledge the late Professor Dan J. Stein for his longstanding leadership and collaboration within the ENIGMA-Bipolar Disorder Working Group, and for his invaluable contributions to psychiatry, neuroscience, and mental health reserach. His intellectual generosity, mentorship, and unwavering support shaped this work and influenced the broader field in lasting ways. His scientific legacy and his kindness to colleagues continue to inspire us.

EV received grants and served as consultant, advisor, or continuing medical education (CME) speaker for the following entities (unrelated to the current work): AB-Biotics, Abbott, AbbVie, Aimentia, Angelini, Biogen, Biohaven, Boehringer Ingelheim, Casen-Recordati, Celon, Compass, Dainippon Sumitomo Pharma, Ethypharm, Ferrer, Gedeon Richter, GH Research, Glaxo Smith-Kline, Idorsia, Janssen, Lundbeck, Novartis, Organon, Otsuka, Rovi, Sage, Sanofi-Aventis, Sunovion, Takeda, and Viatris. JRa received CME honoraria from Inspira Networks for a machine learning course promoted by Adamed outside the submitted work. JRe received speaker's honoraria from Janssen, Hexal, Neuraxpharm, and Novartis. OAA is a consultant for Cortechs.ai and Precision Health and has received speaker's honoraria from Lundbeck, BMS, Lilly, Janssen, and Otsuka. All other authors report no biomedical financial interests or potential conflicts of interest.

## ARTICLE INFORMATION

From the Imaging Genetics Center, Mark and Mary Stevens Neuroimaging and Informatics Institute, Keck School of Medicine of University of Southern California, University of Southern California, Marina del Rey, California (LN, MJYK, NJ, SIT, PMT, CRKC); Clinical Neuroimaging Laboratory, Centre for Neuroimaging, Cognition and Genomics, Galway Neuroscience Centre, College of Medicine Nursing and Health Sciences, University of Galway, Galway, Ireland (LN, GM, FMM, CM, BHal, SO, DMC); Department of Psychiatry, University Medical Center Groningen, University of Groningen, Groningen, the Netherlands (BHaa); Neuroscience Institute, University of Cape Town, Cape Town, South Africa (DJS, FSc), Department of Psychiatry and Mental Health, University of Cape Town, Cape Town, South Africa (DJS, FMH, FSc, HST); South African Medical Research Council Unit on Risk and Resilience in Mental Disorders, University of Cape Town, Cape Town, South Africa (DJS); Department of Psychiatry, Boston Children's Hospital and Harvard Medical School, Boston, Massachusetts (DCG, AR); Biomedical Research Networking Center for Mental Health Network, Instituto de Salud Carlos III, Madrid, Spain (EP-C, EV, JRa, RS, AK, EJC-R); FIDMAG Germanes Hospitalàries Research Foundation, Barcelona, Spain (EP-C, JRa, RS, AK, EJC-R); Institut d'Investigacions Biomèdiques August Pi i Sunyer, Barcelona, Spain (EV, JRa); Barcelona Bipolar Disorders and Depressive Unit, Hospital Clínic, Institute of Neurosciences, University of Barcelona, Barcelona, Spain (EV, JRa); Signal Processing Laboratory, École Polytechnique Fédérale de Lausanne, Lausanne, Switzerland (EJC-R); Northern Health, Mental Health Division, and the University of Melbourne, Melbourne, Victoria, Australia (JH); Institut National de la Santé et de la Recherche Médicale U955, team "Translational Neuro-Psychiatry," Créteil, France (PF); Neurospin, CEA Paris-Saclay, team UNIACT, Gif-sur-Yvette, France (PF); University Grenoble Alpes, Centre Hospitalier Universitaire Grenoble Alpes, Grenoble, France (MP, AP); Institut National de la Santé et de la Recherche Médicale U1216, Grenoble Institut des Neurosciences, La Tronche, France (MP, AP); Department of Pathophysiology and Transplantation, University of Milan, Milan, Italy (PB); Department of Neurosciences and Mental Health, Fondazione Istituto di Ricovero e Cura a Carattere Scientifico Ca' Granda Ospedale Maggiore Policlinico, Milan, Italy (PB); Section of Psychiatry, Department of Neurosciences, Biomedicine and Movement Sciences, University of Verona, Verona, Italy (MBel); Discipline of Psychiatry and Mental Health, School of Clinical Medicine, University of New South Wales, Sydney, New South Wales, Australia (PBM, GR); Institute for Translational Psychiatry, University of Münster, Münster, Germany (UD, TB, SM, KF, JRe, EJL, DG, TH); Department of Psychiatry, Protestant Hospital of the Bethel Foundation, Medical School and University Medical Center OWL, Bielefeld University, Bielefeld, Germany (UD); Institute for Translational Neuroscience, University of Münster, Münster, Germany (SM); Department of Psychiatry, Psychosomatic Medicine and Psychotherapy, Goethe University Frankfurt, University Hospital, Frankfurt, Germany (JRe); Cooperative Brain Imaging Center, Goethe University Frankfurt, Frankfurt, Germany (JRe); Central Institute of Mental Health, Department of Neuropsychology and Psychological Resilience Research, Mannheim, Germany (MW); DKFZ Hector Cancer Institute at the University Medical Center Mannheim, Mannheim, Germany (MW); Department of Cancer Survivorship and Psychological Resilience, German Cancer Research Center Heidelberg, Heidelberg, Germany (MW); Department of Psychiatry, University of Pittsburgh, Pittsburgh, Pennsylvania (MLP); Department of Psychiatry and Psychotherapy, Faculty of Medicine, Philipps-Universität Marburg, Marburg, Germany (LT, TK, BS, OS, FSt, FT-O, NA, PLU, AJ); Core-Facility Brainimaging, Faculty of Medicine, University of Marburg, Marburg, Germany (AJ); Orygen, The National Centre of Excellence in Youth Mental Health, Parkville, Victoria, Australia (MBer); Centre for Youth Mental Health, University of Melbourne, Parkville, Victoria, Australia (MBer); IMPACT Institute, School of Medicine, Deakin University, Geelong, Victoria, Australia (MBer); Orygen Youth Health Clinical Program, Parkville, Victoria, Australia (MBer); Barwon Health and the Geelong Clinic, Geelong, Victoria, Australia

(MBer); Brain and Mental Health Laboratory, School of Psychological Science and Monash Institute of Cognitive and Clinical Neurosciences, Monash University, Clayton, Victoria, Australia (OD); Melbourne Neuropsychiatry Centre, Department of Psychiatry, The University of Melbourne and Melbourne Health, Carlton South, Victoria, Australia (OD); Centre for Precision Psychiatry, Institute of Clinical Medicine, University of Oslo, Oslo, Norway (NP, OAA); Division of Mental Health and Addiction, Oslo University Hospital, Oslo, Norway (NP, OAA); Turner Institute for Brain and Mental Health, School of Psychological Science and Monash Biomedical Imaging, Monash University, Victoria, Australia (CS); Queensland Institute of Medical Research Berghofer, Berghofer, Queensland, Australia (CS); Healthy Brain and Mind Research Centre, School of Behavioral and Health Sciences, Faculty of Health Sciences, Australian Catholic University, Fitzroy, Victoria, Australia (CS); and School of Psychology, University of Queensland, Brisbane, Queensland, Australia (CS).

Address correspondence to Leila Nabulsi, Ph.D., at lnabulsi@usc.edu.

Received Dec 4, 2025; revised Apr 21, 2026; accepted Apr 24, 2026.

Supplementary material cited in this article is available online at https://doi.org/10.1016/j.biopsych.2026.04.020.

## REFERENCES

1. Vos T, Abajobir AA, Abate KH, Abbafati C, Abbas KM, Abd-Allah F, *et al.* (2017): Global, regional, and national incidence, prevalence, and years lived with disability for 328 diseases and injuries for 195 countries, 1990–2016: A systematic analysis for the Global Burden of Disease Study 2016. Lancet 390:1211–1259.
2. Malhi GS, Tanious M, Das P, Coulston CM, Berk M (2013): Potential mechanisms of action of lithium in bipolar disorder: Current understanding. CNS Drugs 27:135–153.
3. McIntyre RS, Calabrese JR (2019): Bipolar depression: The clinical characteristics and unmet needs of a complex disorder. Curr Med Res Opin 35:1993–2005.
4. Levenberg K, Cordner ZA (2022): Bipolar depression: A review of treatment options. Gen Psychiatry 35:e100760.
5. Chesney E, Goodwin GM, Fazel S (2014): Risks of all-cause and suicide mortality in mental disorders: A meta-review. World Psychiatry 13:153–160.
6. O'Donoghue S, Kilmartin L, O'Hora D, Emsell L, Langan C, McInerney S, *et al.* (2017): Anatomical integration and rich-club connectivity in euthymic bipolar disorder. Psychol Med 47:1609–1623.
7. Ching CRK, Hibar DP, Gurholt TP, Nunes A, Thomopoulos SI, Abé C, *et al.* (2020): What we learn about bipolar disorder from large-scale neuroimaging: Findings and future directions from the ENIGMA Bipolar Disorder Working Group. Hum Brain Mapp 43:56–82.
8. Favre P, Pauling M, Stout J, Hozer F, Sarrazin S, Abé C, *et al.* (2019): Widespread white matter microstructural abnormalities in bipolar disorder: Evidence from mega- and meta-analyses across 3033 individuals. Neuropsychopharmacology 44:2285–2293.
9. Parker N, Ching CRK (2025): Mapping structural neuroimaging trajectories in bipolar disorder: Neurobiological and clinical implications. Biol Psychiatry 98:311–321.
10. Wang F, Kalmar JH, Edmiston EK, Chepenik LG, Bhagwagar Z, Spencer L, *et al.* (2008): Abnormal corpus callosum integrity in bipolar disorder: A diffusion tensor imaging study. Biol Psychiatry 64:730–733.
11. Linke J, King AV, Poupon C, Hennerici MG, Gass A, Wessa M (2013): Impaired anatomical connectivity and related executive functions: Differentiating vulnerability and disease marker in bipolar disorder. Biol Psychiatry 74:908–916.
12. Nabulsi L, Chandio BQ, McPhilemy G, Martyn FM, Roberts G, Hallahan B, *et al.* (2023): Multi-site statistical mapping of along-tract microstructural abnormalities in bipolar disorder with diffusion MRI tractometry. Presented at 19th International Symposium on Medical Information Processing and Analysis (SIPAIM), 1–5.
13. Sarrazin S, Poupon C, Linke J, Wessa M, Phillips M, Delavest M, *et al.* (2014): A multicenter tractography study of deep white matter tracts in bipolar I disorder: Psychotic features and interhemispheric disconnectivity. JAMA Psychiatry 71:388–396.
14. Sporns O (2013): The human connectome: Origins and challenges. Neuroimage 80:53–61.
15. Perry A, Roberts G, Mitchell PB, Breakspear M (2018): Connectomics of bipolar disorder: A critical review, and evidence for dynamic instabilities within interoceptive networks. Mol Psychiatry 24:1296–1318.
16. Hibar DP, Westlye LT, Van Erp TGM, Rasmussen J, Leonardo CD, Faskowitz J, *et al.* (2016): Subcortical volumetric abnormalities in bipolar disorder. Mol Psychiatry 21:1710–1716.
17. Hibar DP, Westlye LT, Doan NT, Jahanshad N, Cheung JW, Ching CRK, *et al.* (2017): Cortical abnormalities in bipolar disorder: An MRI analysis of 6503 individuals from the ENIGMA Bipolar Disorder Working Group. Mol Psychiatry 23:932–942.
18. Thompson PM, Jahanshad N, Ching CRK, Salminen LE, Thomopoulos SI, Bright J, *et al.* (2020): ENIGMA and global neuroscience: A decade of large-scale studies of the brain in health and disease across more than 40 countries. Transl Psychiatry 10:100.
19. Pierpaoli C, Jezzard P, Basser PJ, Barnett A, Di Chiro G (1996): Diffusion tensor MR imaging of the human brain. Radiology 201:637–648.
20. Fornito A, Zalesky A, Bullmore E (2016): Fundamentals of Brain Network Analysis. Academic press.
21. Nabulsi L, McPhilemy G, Kilmartin L, O'Hora D, O'Donoghue S, Forcellini G, *et al.* (2019): Bipolar disorder and gender are associated with frontolimbic and basal ganglia dysconnectivity: A study of topological variance using network analysis. Brain Connect 9:745–759.
22. Fischl B (2012): FreeSurfer. NeuroImage 62:774–781.
23. Desikan RS, Ségonne F, Fischl B, Quinn BT, Dickerson BC, Blacker D, *et al.* (2006): An automated labeling system for subdividing the human cerebral cortex on MRI scans into gyral based regions of interest. Neuroimage 31:968–980.
24. Leemans A, Jeurissen B, Sijbers J, Jones D (2009): ExploreDTI: A graphical toolbox for processing, analyzing, and visualizing diffusion MR data. Proceedings of the 17th Scientific Meeting, International Society for Magnetic Resonance in Medicine 17:3537.
25. Tournier J-D, Calamante F, Connelly A (2007): Robust determination of the fibre orientation distribution in diffusion MRI: Non-negativity constrained super-resolved spherical deconvolution. Neuroimage 35:1459–1472.
26. Nabulsi L, Mcphilemy G, O'donoghue S, Cannon DM, Kilmartin L, O'hora D, *et al.* (2022): Aberrant subnetwork and hub dysconnectivity in adult bipolar disorder: A multicenter graph theory analysis. Cereb Cortex 32:2254–2264.
27. Rubinov M, Sporns O (2010): Complex network measures of brain connectivity: Uses and interpretations. Neuroimage 52:1059–1069.
28. Benjamini Y, Hochberg Y (1995): Controlling the false discovery rate: A practical and powerful approach to multiple testing. J R Stat Soc B 57:289–300.
29. Zalesky A, Fornito A, Bullmore ET (2010): Network-based statistic: Identifying differences in brain networks. Neuroimage 53:1197–1207.
30. Worley L (2017): Neuroscience-based nomenclature (NbN). Lancet Psychiatry 4:272–273.
31. van den Heuvel MP, Sporns O (2013): An anatomical substrate for integration among functional networks in human cortex. J Neurosci 33:14489–14500.
32. Sha Z, Wager TD, Mechelli A, He Y (2019): Common dysfunction of large-scale neurocognitive networks across psychiatric disorders. Biol Psychiatry 85:379–388.
33. Adler CM, DelBello MP, Strakowski SM (2006): Brain network dysfunction in bipolar disorder. CNS Spectr 11:312–320.
34. Strakowski SM, Adler CM, Almeida J, Altshuler LL, Blumberg HP, Chang KD, *et al.* (2012): The functional neuroanatomy of bipolar disorder: A consensus model. Bipolar Disord 14:313–325.
35. Leow A, Ajilore O, Zhan L, Arienzo D, Gadelkarim J, Zhang A, *et al.* (2013): Impaired inter-hemispheric integration in bipolar disorder revealed with brain network analyses. Biol Psychiatry 73:183–193.
36. Gadelkarim JJ, Ajilore O, Schonfeld D, Zhan L, Thompson PM, Feusner JD, *et al.* (2014): Investigating brain community structure

abnormalities in bipolar disorder using path length associated community estimation. Hum Brain Mapp 35:2253–2264.
37. Roberts G, Perry A, Lord A, Frankland A, Leung V, Holmes-Preston E, *et al.* (2018): Structural dysconnectivity of key cognitive and emotional hubs in young people at high genetic risk for bipolar disorder. Mol Psychiatry 23:413–421.
38. Wang Y, Deng F, Jia Y, Wang J, Zhong S, Huang H, *et al.* (2018): Disrupted rich club organization and structural brain connectome in unmedicated bipolar disorder. Psychol Med 49:510–518.
39. Allen EA, Erhardt EB, Damaraju E, Gruner W, Segall JM, Silva RF, *et al.* (2011): A baseline for the multivariate comparison of resting-state networks. Front Syst Neurosci 5:2.
40. Sun Y, Lee R, Chen Y, Collinson S, Thakor N, Bezerianos A, Sim K (2015): Progressive gender differences of structural brain networks in healthy adults: A longitudinal, diffusion tensor imaging study. PLoS One 10:e0118857.
41. Suwalska A, Łojko D (2014): Sex dependence of cognitive functions in bipolar disorder. Sci World J 2014:1–10.
42. Zovetti N, Rossetti MG, Perlini C, Maggioni E, Bontempi P, Bellani M, Brambilla P (2020): Default mode network activity in bipolar disorder. Epidemiol Psychiatr Sci 29:e166.
43. Jones DK, Knösche TR, Turner R (2013): White matter integrity, fiber count, and other fallacies: The do's and don'ts of diffusion MRI. Neuroimage 73:239–254.
44. Yeh F-C, Panesar S, Fernandes D, Meola A, Yoshino M, Fernandez-Miranda JC, *et al.* (2018): Population-averaged atlas of the macroscale human structural connectome and its network topology. Neuroimage 178:57–68.
45. Patel Y, Parker N, Shin J, Howard D, French L, Thomopoulos SI, *et al.* (2021): Virtual histology of cortical thickness and shared neurobiology in 6 psychiatric disorders. JAMA Psychiatry 78:47–63.
46. Park B, Kebets V, Larivière S, Hettwer MD, Paquola C, van Rooij D, *et al.* (2022): Multiscale neural gradients reflect transdiagnostic effects of major psychiatric conditions on cortical morphology. Commun Biol 5:1024.
47. Ajilore O, Vizueta N, Walshaw P, Zhan L, Leow A, Altshuler LL (2015): Connectome signatures of neurocognitive abnormalities in euthymic bipolar I disorder. J Psychiatr Res 68:37–44.
48. Sporns O (2011): The human connectome: A complex network. Ann N Y Acad Sci 1224:109–125.
49. Bassett DS, Sporns O (2017): Network neuroscience. Nat Neurosci 20:353–364.
50. Uddin LQ, Supekar KS, Ryali S, Menon V (2011): Dynamic reconfiguration of structural and functional connectivity across core neurocognitive brain networks with development. J Neurosci 31:18578–18589.
51. Mesulam M, Mufson EJ (1982): Insula of the Old World Monkey. Architectonics in the Insulo-orbito- temporal component of the paralimbic brain 22:1–22.
52. Nabulsi L, Farrell J, McPhilemy G, Kilmartin L, Dauvermann MR, Akudjedu TN, *et al.* (2022): Normalization of impaired emotion inhibition in bipolar disorder mediated by cholinergic neurotransmission in the cingulate cortex. Neuropsychopharmacology 47:1643–1651.
53. Barch DM (2005): The cognitive neuroscience of schizophrenia. Annu Rev Clin Psychol 1:321–353.
54. Phillips ML, Ladouceur CD, Drevets WC (2008): Neural systems underlying voluntary and automatic emotion regulation: Toward a neural model of bipolar disorder. Mol Psychiatry 13:829.
55. Menon V (2015): Salience network. In: Brain Mapping, vol. 2: Amsterdam: Elsevier Incorporated, 597–611.
56. Benedetti F, Poletti S, Hoogenboezem TA, Mazza E, Ambrée O, de Wit H, *et al.* (2016): Inflammatory cytokines influence measures of white matter integrity in bipolar disorder. J Affect Disord 202:1–9.
57. Joslyn C, Hawes DJ, Hunt C, Mitchell PB (2016): Is age of onset associated with severity, prognosis, and clinical features in bipolar disorder? A meta-analytic review. Bipolar Disord 18:389–403.
58. Vieta E, Berk M, Schulze TG, Carvalho AF, Suppes T, Calabrese JR, *et al.* (2018): Bipolar disorders. Nat Rev Dis Prim 4:1–16.
59. Houenou J, Wessa M, Douaud G, Leboyer M, Chanraud S, Perrin M, *et al.* (2007): Increased white matter connectivity in euthymic bipolar patients: Diffusion tensor tractography between the subgenual cingulate and the amygdalo-hippocampal complex. Mol Psychiatry 12:1001–1010.
60. Manji HK, Quiroz JA, Payne JL, Singh J, Lopes BP, Viegas JS, Zarate CA (2003): The underlying neurobiology of bipolar disorder. World Psychiatry 2:136.
61. Abé C, Ching CRK, Liberg B, Lebedev AV, Agartz I, Akudjedu TN, *et al.* (2022): Longitudinal structural brain changes in bipolar disorder: A multicenter neuroimaging study of 1232 individuals by the ENIGMA bipolar disorder working group. Biol Psychiatry 91:582–592.
62. Vieta E, De Prisco M (2024): Cross-sectional studies: Is pressing the pause button worth it in research? Eur Neuropsychopharmacol 85:32–33.
63. Godlewska BR, Norbury R, Selvaraj S, Cowen PJ, Harmer CJ (2012): Short-term SSRI treatment normalises amygdala hyperactivity in depressed patients. Psychol Med 42:2609–2617.
64. Spielberg JM, Matyi MA, Karne H, Anand A (2019): Lithium monotherapy associated longitudinal effects on resting state brain networks in clinical treatment of bipolar disorder. Bipolar Disord 21:361–371.
65. Schmaal L, Pozzi E, Ho C, Van Velzen LS, Veer IM, Opel N, *et al.* (2020): ENIGMA MDD: Seven years of global neuroimaging studies of major depression through worldwide data sharing. Transl Psychiatry 10:172.
66. Meador KJ (2003): Newer anticonvulsants: Dosing strategies and cognition in treating patients with mood disorders and epilepsy. J Clin Psychiatry 64:30–34.
67. Jeurissen B, Descoteaux M, Mori S, Leemans A (2019): Diffusion MRI fiber tractography of the brain. NMR Biomed 32:e3785.
68. Jones DK, Cercignani M (2010): Twenty-five pitfalls in the analysis of diffusion MRI data. NMR Biomed 23:803–820.